

---

*Research article*

# **Modeling and optimization of the tribological properties of an epoxy resin reinforced with nano graphene oxide nano $\text{Al}_2\text{O}_3/\text{MoS}_2$ particles by RSM**

**Olfat Ahmed Mahmood**

Collage of Sciences, Diyala University, Diyala, Iraq

\* **Correspondence:** Email: [olfat@uodiyala.edu.iq](mailto:olfat@uodiyala.edu.iq); Tel: +964-771-961-3384.

**Abstract:** The tribological properties of epoxy resin, a thermosetting polymer, were enhanced through the incorporation of nano- and micro-scale fillers. A hybrid composite was developed by dispersing nano-alumina and micro-molybdenum disulfide ( $\text{MoS}_2$ ) within an epoxy matrix pre-modified with nano-graphene oxide. Specimen preparation was conducted via a laboratory ball mill, and a response surface methodology was utilized to optimize filler weight fractions. Evaluation via pin-on-disc testing (ASTM G99) under dry sliding conditions verified the improvement in tribological characteristics. The optimal formulation, containing 0.5 wt% graphene oxide, 3.92 wt% nano-alumina, and 3.99 wt%  $\text{MoS}_2$ , yielded a minimal coefficient of friction (0.12) and a low wear rate ( $2.3 \times 10^{-6} \text{ mm}^3/\text{N}\cdot\text{m}$ ). Furthermore, this composite retained commendable mechanical properties, with a tensile strength of 75.4 MPa and a modulus of elasticity of 3.1 GPa.

**Keywords:** nano epoxy; nano graphene; coefficient of friction; wear rate; surface response method

---

## **1. Introduction**

Composites exhibit excellent characteristics, such as low weight, high strength, and resistance to impact, heat, and wear. They are stronger as a combined system than as individual components [1,2]. Composite materials consist of three basic physical phases: the matrix phase, the reinforcement phase, and the interphase [3].

There are several reasons for adding materials to a matrix to create composites with special performance characteristics. One reason is to increase the mechanical properties of polymers, as fibers or particulates can be used to improve their performance [1,2]. A second reason is to improve tribological properties by reducing the coefficient of friction and wear rate (self-lubricating composites) [4]. Another reason is to increase the thermal properties of composites. Because polymers generally exhibit low thermal conductivity, the addition of special additives helps reduce the heat generated during sliding contact [1–3]. Self-lubricating composites are greatly affected by various factors, including temperature, speed, normal load, and environmental conditions. Therefore, polymers are modified with nano- and micro-sized additives to enhance their overall performance [5]. Nanomaterials offer several advantages, including improved durability, resistance to chemical and mechanical degradation, enhanced thermal properties, and better moisture resistance. Due to their large surface area, nanomaterials exhibit remarkable physical and chemical properties, although they tend to form agglomerates [1,6–8]. Epoxy systems are one of the most important thermosetting materials, frequently used in demanding applications [9].

In general, nanoparticles must be uniformly dispersed, rather than agglomerated, to achieve optimal material properties. Agglomeration is a common challenge in polymer nanocomposites, especially at higher nanofiller contents. To date, various inorganic nanoparticles, e.g.,  $\text{Al}_2\text{O}_3$ ,  $\text{TiO}_2$ ,  $\text{ZnO}$ ,  $\text{CuO}$ ,  $\text{SiC}$ ,  $\text{ZrO}_2$ ,  $\text{Si}_3\text{N}_4$ ,  $\text{SiO}_2$ , and  $\text{CaCO}_3$ , have been incorporated into both thermoset and thermoplastic matrices to improve wear resistance [1,2,10,11].

Previous studies using only nanoparticles, such as silicon nitride or zirconia, succeeded in enhancing the wear resistance of epoxy. However, excessive addition led to particle agglomeration [8,12]. On the other hand, using larger microparticles, such as molybdenum disulfide ( $\text{MoS}_2$ ), reduced friction but weakened the composite mechanically [1]. Even when researchers combined materials like titanium dioxide with carbon nanotubes or graphene with  $\text{MoS}_2$ , fillers were usually of similar sizes [2,13]. A major limitation of epoxy resin is its high friction and susceptibility to wear, which restricts its use in moving components [1,2].

Our research addresses these issues with a novel approach: we mix nano-sized graphene oxide (GO) and alumina with micro-sized  $\text{MoS}_2$  into an epoxy matrix. Using statistical methods to find the best composition, we developed a composite that is slippery, highly wear-resistant, and mechanically strong, successfully overcoming traditional trade-offs.

## 2. Materials and methods

### 2.1. Material

The epoxy resin used was Araldite LY 5052, combined with the Aradur 5052 hardener, supplied by Huntsman Germany (Table 1). The additives included graphene oxide nanoparticles (8 layers, purity 99%, surface area  $>120 \text{ g/m}^2$ ) obtained from Nano Tech Company (India), nano-alumina particles (50 nm, purity 99.9%) from Nano Elements Company (India), and  $\text{MoS}_2$  particles ( $<40 \text{ }\mu\text{m}$ , purity 99%) from Xinhai Company (China).

**Table 1.** Technical data sheet for epoxy resin with its hardener.

Individual components	Mixing (parts by weight)	ratio by (parts by volume)	Viscosity, 25 °C (mPa·s)	Density, 25 °C (g/cm <sup>3</sup> )	Potlife, 100 g/RT (approx. values (min))	Mixed viscosity, 25 °C (mPa·s)
Araldite 5052	LY 100	100	~1500	1.17	160	700
Aradur 5052	38	47	<60	0.94		

## 2.2. Design of experiment and model development by response surface method (RSM)

The RSM is a widely used mathematical and statistical method for modeling and analyzing experimental data, where a dependent variable is influenced by several independent factors with the aim of optimizing the response.

RSM quantifies the relationships between the response variable (Y) and the input variables ( $x_1$ ,  $x_2$ , ...,  $x_k$ ). If these input variables are controlled and randomized in the experiment, and error is minimal, the response (Y) can be expressed as Eq 1:

$$Y = f(x_1, x_2, \dots) + c \quad (1)$$

In this research, three influencing factors were examined using the RSM. Two materials were added to an epoxy resin modified with graphene oxide in varying amounts, and their effects on the coefficient of friction (COF) and wear rate were analyzed using Minitab software. The experimental data were used to determine the main and interaction effects of the variables and to optimize the additive composition for improved tribological performance.

The selection of 0.5 wt% GO was based on initial experimental results and previous literature. As shown in Table 2, while 0.1 wt% GO showed minimal improvement, 0.5 wt% led to a significant enhancement in both tensile strength and tribological properties. Increasing the GO content to 1.0 wt% led to reduced performance due to agglomeration of GO sheets [14,15]. Tang et al. [14] reported that 0.5 wt% GO achieved the best dispersion and mechanical reinforcement in epoxy composites, beyond which properties plateaued or deteriorated.

Table 2 presents the design of experiments based on the surface response method, considering two variable factors: nano- $\text{Al}_2\text{O}_3$  and  $\text{MoS}_2$  particle contents.

**Table 2.** RSM for epoxy resin and additives.

Run order	Epoxy resin with 0.5 wt% nano-GO	Nano-Al <sub>2</sub> O <sub>3</sub> (wt%)	MoS <sub>2</sub> (wt%)
1	100	4.00	2.50
2	100	3.41	4.27
3	100	2.00	2.50
4	100	2.00	2.50
5	100	2.00	2.50
6	100	0.59	4.27
7	100	3.41	0.73
8	100	2.00	0.00
9	100	2.00	2.50
10	100	2.00	2.50
11	100	0.00	2.50
12	100	2.00	5.00
13	100	0.59	0.73

### 2.3. Specimen preparation and compositions

Homogeneous nano-epoxy composite specimens were prepared according to Table 2 following a mixing procedure, as described below.

#### 2.3.1. Preparing nanocomposite resin

To remove absorbed moisture and reduce agglomeration, powders were dried at 140 °C (4 h for GO and nano-alumina and 3 h for MoS<sub>2</sub>), placed in a container (200 mL), ground using a ball mill for 12 h, and dried again at 150 °C for 2 h.

Homogeneous dispersion of nanofillers is critical for performance enhancement. The ball-milling process was employed to overcome van der Waals forces and prevent agglomeration. The improvement in tensile strength (from 65 to 75.4 MPa) and the low wear rate ( $2.3 \times 10^{-6}$  mm<sup>3</sup>/N·m) provide strong evidence of effective dispersion and interfacial adhesion. Mechanical and tribological test results confirmed that the fillers were well-distributed and strongly bonded to the epoxy matrix, facilitating efficient stress transfer and the formation of a stable protective tribofilm during sliding.

The resin was weighed, placed in a glass container with ten steel pellets (three pellets with a diameter of 6 mm and seven with 8 mm), and heated to 60 °C to reduce viscosity, ensuring uniform dispersion of the nanocomposite. Additives were gradually added to the resin in ten steps and carefully mixed using a laboratory ball mill for 7 h at 60 °C and 200 rpm. After mixing, the mixture was placed in the oven at 60 °C for 1 h and mixed again using a ball mill for 2 h without heat and pellets. The resulting nano-epoxy composite was homogeneous.

### 2.3.2. Casting and post-curing

The specimens were evacuated using a vacuum pump for 20 min to eliminate air bubbles. The hardener was then added at a stoichiometric ratio under atmospheric conditions and stirred manually using a wooden stick. After thorough mixing, the mixture was evacuated again for 15 min, then poured into silicon rubber molds and left to cure at room temperature for 7 days. Finally, the composites were post-cured at 50 °C for 3 h. The dimensions of the wear specimens were prepared according to ASTM G99 [16].

### 2.4. Test details

A pin-on-disc wear test apparatus is a test instrument designed for precise and repeatable tribological characterization of bulk materials, coatings, and lubricants. This test was used in our research for dry sliding wear experiments.

After post-curing, the epoxy nanocomposite specimens were sanded with 700, 1000, and 2000 sandpaper. Tests were conducted under dry sliding conditions against a smooth steel pin, at a constant velocity of 0.1 m/s, normal load of 30 N, distance of 500 m, and ambient conditions ( $23 \pm 2$  °C and  $55\% \pm 5\%$  relative humidity), in accordance with ASTM G99 [16]. Circular samples were prepared as disks with dimensions  $40 \times 10$  mm, while the counterface pin was made of steel (50/00, 800 Vickers), as shown in Figure 1.



**Figure 1.** Tribometer instrument.

The coefficient of friction ( $\mu$ ) and wear rate ( $ws$ ) were calculated from the measured data as presented in Eqs 2 and 3, respectively:

$$\mu = \frac{F_R}{F_N} \quad (2)$$

where  $F_R$  is the friction force, and  $F_N$  is the normal load.

$$WS = \frac{\Delta m}{\rho \cdot F_N \cdot l} = \frac{\Delta v}{F_N \cdot l} \quad (3)$$

$\Delta m$  is the mass loss,  $\rho$  is the density of the composite specimens,  $\Delta v$  is the volume loss, and  $l$  is the sliding distance. Tensile tests were carried out using a universal testing machine (model STM150) in accordance with ASTM D638, at room temperature, using a 2000 kg load cell and a speed rate of 2 mm/min.

### 3. Results and discussion

#### 3.1. Effect of nanographene oxide on the mechanical and tribological properties

GO exhibits good compatibility and dispersibility within epoxy resin, owing to its large specific surface area and high mechanical strength resulting from the pleated structure on its surface [14,15]. Nanographene oxide powder was added to the epoxy resin to improve its mechanical and tribological properties by improving load transfer and inhibiting crack propagation. Table 3 presents the average of three measurements for both mechanical and tribological property tests of the graphene oxide–epoxy composite specimens.

**Table 3.** Tribological and mechanical properties for epoxy resin and graphene oxide–epoxy composite.

Epoxy resin (g)*	GO (g)	Density (g/cm <sup>3</sup> )	Tensile strength (MPa)	Young modulus (GPa)	COF	Wear rate ( $\times 10^{-6}$ mm <sup>3</sup> /N·m)
100	0	1.14	65 $\pm$ 3	2.6 $\pm$ 0.1	0.71 $\pm$ 0.02	180 $\pm$ 5
100	0.1	1.14	72 $\pm$ 2	2.6 $\pm$ 0.1	0.62 $\pm$ 0.03	120 $\pm$ 4
100	0.5	1.15	90 $\pm$ 2	2.8 $\pm$ 0.1	0.5 $\pm$ 0.01	90 $\pm$ 2
100	1	1.17	80 $\pm$ 2	2.9 $\pm$ 0.1	0.055 $\pm$ 0.01	104 $\pm$ 2

\*Note: Weight of the mixture of epoxy resin with hardener.

In general, the tensile strength and elastic modulus improved by 38.5% and 7.7%, respectively. The coefficient of friction and wear rate for the graphene oxide–epoxy composites were reduced by 19.4% and 50%, respectively. The presence of the graphene oxide smooths the surface topography of composites [2,17]. Moreover, graphene oxide promotes the formation of transfer films that separate the specimen surface from the counterface, thereby reducing debris generation and friction stress.

#### 3.2. Synergy of GO, nano-alumina oxide, and MoS<sub>2</sub> particles

In order to improve the tribological properties of the epoxy resin, nano-alumina and MoS<sub>2</sub> were added to the epoxy resin previously modified with nano-graphene oxide particles. The experimental data for the coefficient of friction and wear rate are presented in Table 4, and their analysis was

performed using the surface response method in Minitab software. Thirteen experiments were conducted at different combinations of the factors, and the central point was repeated five times to determine the synergistic effects of the nano- and microparticles.

**Table 4.** Tribological properties for nano-epoxy composite (surface response method).

Run order	Epoxy resin (g)	GO (wt%)	Al <sub>2</sub> O <sub>3</sub> (wt%)	MoS <sub>2</sub> (wt%)	Density (g/cm <sup>3</sup> )	COF	Wear rate (mm <sup>3</sup> /N·m)
1	100	0.50	4.00	2.50	1.27	0.15	$2.5 \times 10^{-6}$
2	100	0.50	3.41	4.27	1.3	0.11	$10 \times 10^{-6}$
3	100	0.50	2.00	2.50	1.22	0.20	$4.0 \times 10^{-5}$
4	100	0.50	2.00	2.50	1.22	0.21	$4.1 \times 10^{-5}$
5	100	0.50	2.00	2.50	1.22	0.23	$3.9 \times 10^{-5}$
6	100	0.50	0.58	4.27	1.17	0.20	$6.0 \times 10^{-5}$
7	100	0.50	3.41	0.73	1.24	0.27	$1.5 \times 10^{-5}$
8	100	0.50	2.00	0.00	1.16	0.44	$5.0 \times 10^{-5}$
9	100	0.50	2.00	2.50	1.22	0.21	$4.1 \times 10^{-5}$
10	100	0.50	2.00	2.50	1.22	0.20	$4.0 \times 10^{-5}$
11	100	0.50	0.00	2.50	1.18	0.39	$7.7 \times 10^{-5}$
12	100	0.50	2.00	5.00	1.28	0.14	$3.5 \times 10^{-5}$
13	100	0.50	0.58	0.73	1.15	0.50	$7.8 \times 10^{-5}$

### 3.2.1. ANOVA and model fitting for the coefficient of friction

Tables 3 and 4 demonstrate that COF was reduced from 0.5 to 0.11 (i.e., about 78%) by adding nano-Al<sub>2</sub>O<sub>3</sub> and MoS<sub>2</sub> particles. ANOVA analysis for experimental data is shown in Table 5. The factors Al<sub>2</sub>O<sub>3</sub>, MoS<sub>2</sub>, Al<sub>2</sub>O<sub>3</sub> × Al<sub>2</sub>O<sub>3</sub>, MoS<sub>2</sub> × MoS<sub>2</sub>, and MoS<sub>2</sub> × Al<sub>2</sub>O<sub>3</sub> significantly influenced the coefficient of friction. An R<sup>2</sup> value of 0.9936 (i.e., very close to 1) indicates an excellent fit of the model to the experimental data, while the R<sup>2</sup> (adj) value of 0.9891 suggests that the model is adequate without the need for additional tests. These results can therefore be used to model the design space. p-values less than 0.05 indicate that the model terms are significant. Values greater than 0.10 indicate that model terms are not significant.

The model above was used to predict the coefficient of friction for nano-epoxy composites as a function of nano-alumina oxide and MoS<sub>2</sub>; it can be presented in terms of independent factors, as in Eq 4.

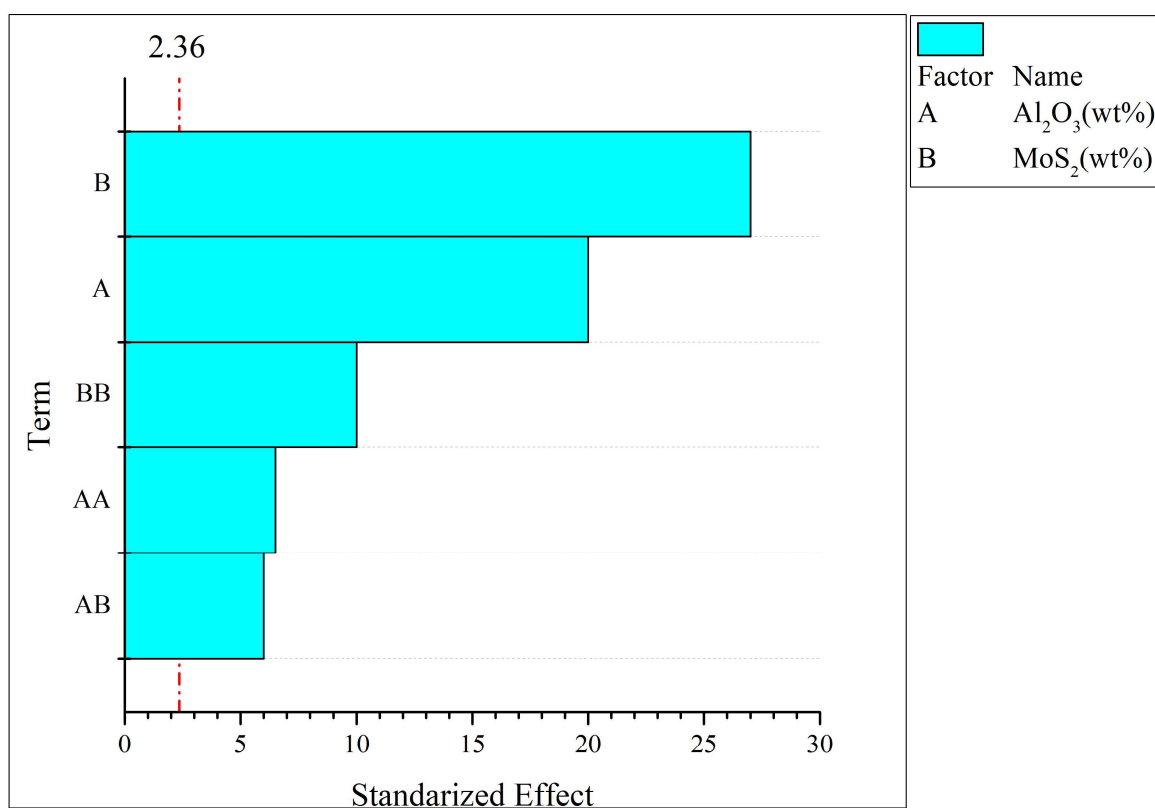
$$\text{COF} = 0.6833 - 0.1438 \text{ Al}_2\text{O}_3 - 0.15177 \text{ MoS}_2 + 0.01304 \text{ Al}_2\text{O}_3 \times \text{Al}_2\text{O}_3 + 0.01231 \text{ MoS}_2 \times \text{MoS}_2 + 0.013 \text{ Al}_2\text{O}_3 \times \text{MoS}_2 \quad (4)$$

Eq 4 and Figure 2 show that MoS<sub>2</sub>, Al<sub>2</sub>O<sub>3</sub>, and MoS<sub>2</sub> × MoS<sub>2</sub> are significant factors for COF.

**Table 5.** Analysis of variance for COF.

Source	DF <sup>(1)</sup>	Adj SS <sup>(2)</sup>	Adj MS <sup>(3)</sup>	F-value	P-value	
Model	5	0.176711	0.035342	218.22	0.001	
Linear	2	0.159048	0.079524	491.02	0.001	
Al <sub>2</sub> O <sub>3</sub>	1	0.056014	0.056014	345.85	0.001	Highly significant
MoS <sub>2</sub>	1	0.103034	0.103034	636.18	0.001	Highly significant
Square	2	0.013438	0.006719	41.49	0.001	
Al <sub>2</sub> O <sub>3</sub> × Al <sub>2</sub> O <sub>3</sub>	1	0.004729	0.004729	29.20	0.001	Significant
MoS <sub>2</sub> × MoS <sub>2</sub>	1	0.010302	0.010302	63.61	0.001	Highly significant
2-way interaction	1	0.004225	0.004225	26.09	0.001	
Al <sub>2</sub> O <sub>3</sub> × MoS <sub>2</sub>	1	0.004225	0.004225	26.09	0.001	Significant
Error	7	0.001134	0.000162			
Lack-of-fit	3	0.000585	0.000195	1.42	0.361	Non-significant
Pure error	4	0.000549	0.000137			
Total	12	0.177845				

Note: (1): Degrees of freedom; (2): adjusted sum of squares; (3): adjusted mean square. Model summary: R<sup>2</sup>, 0.9936; R<sup>2</sup> (adj), 0.9891.

**Figure 2.** Pareto chart of standardized effects on COF.



The COF values for different amounts of nano- $\text{Al}_2\text{O}_3$  and  $\text{MoS}_2$  particles were studied using contour plots and main effect plots (Figure 3). The contour plot allows prediction of COF values for various additive concentrations. COF can be reduced below 0.2 by adding 1.2 wt% nano- $\text{Al}_2\text{O}_3$  and 4–5 wt%  $\text{MoS}_2$ , whereas it can exceed 0.6 by adding 0.3 and 0.2 wt%, respectively. The main effect plot shows that increasing nano- $\text{Al}_2\text{O}_3$  and  $\text{MoS}_2$  particles beyond 4 and 4.8 wt%, respectively, does not significantly change the COF.

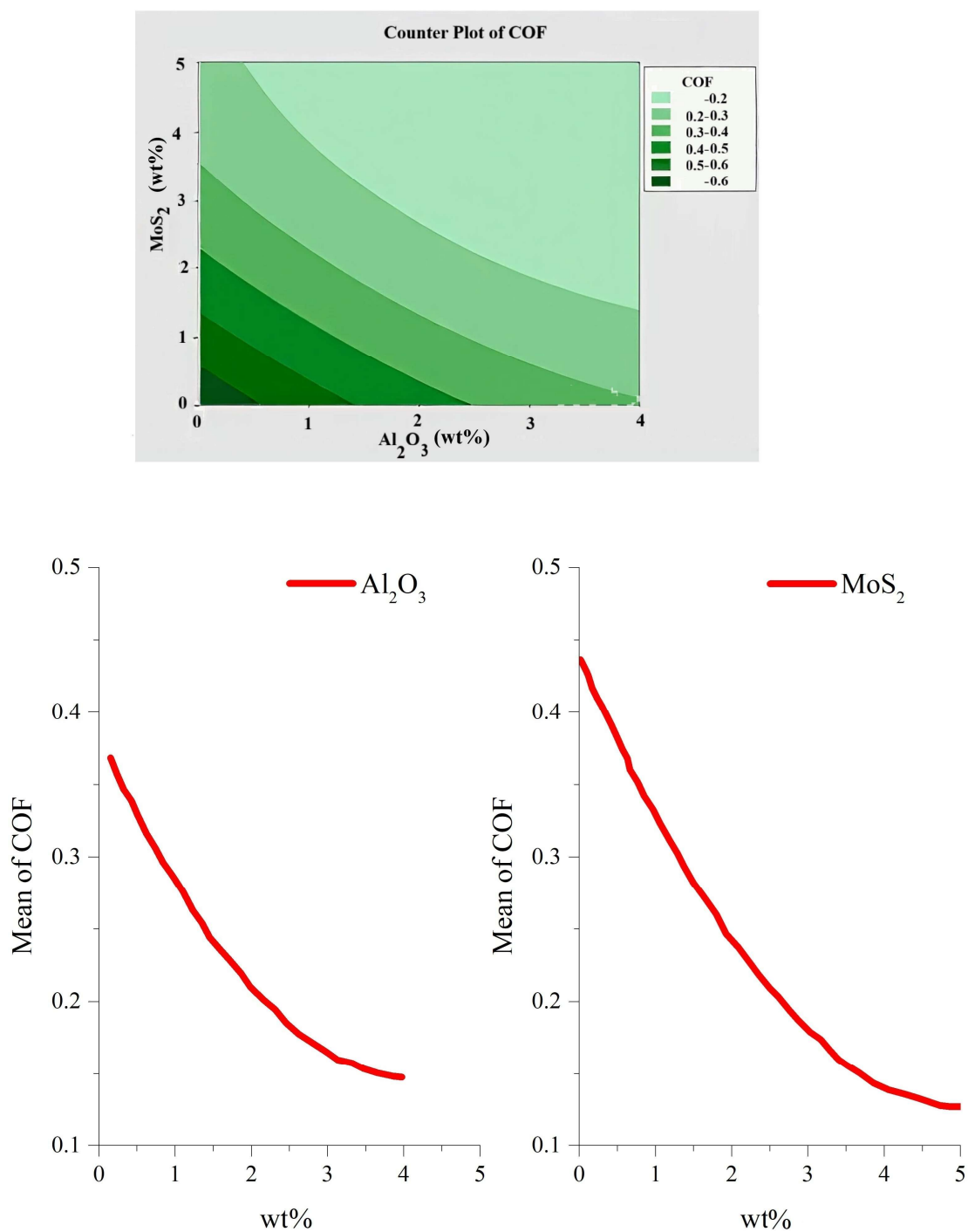


**Figure 3.** Contour plot and main effects plot for COF.

An interaction plot is used to show how the relationship between one factor and a continuous response depends on the level of a second factor.

As shown in Figure 4a, when 0.73 wt% MoS<sub>2</sub> is added and the amount of Al<sub>2</sub>O<sub>3</sub> is varied, the COF reduces drastically to less than 0.3; with 2.5 wt%, it drops further to 0.2 and then gradually levels off to below 0.2. Figure 4b shows that by adding 0.59 wt% of Al<sub>2</sub>O<sub>3</sub> and varying the MoS<sub>2</sub> amounts, the COF reduces drastically to 0.2; the addition of 3.41 wt% reduces it to less than 0.13.

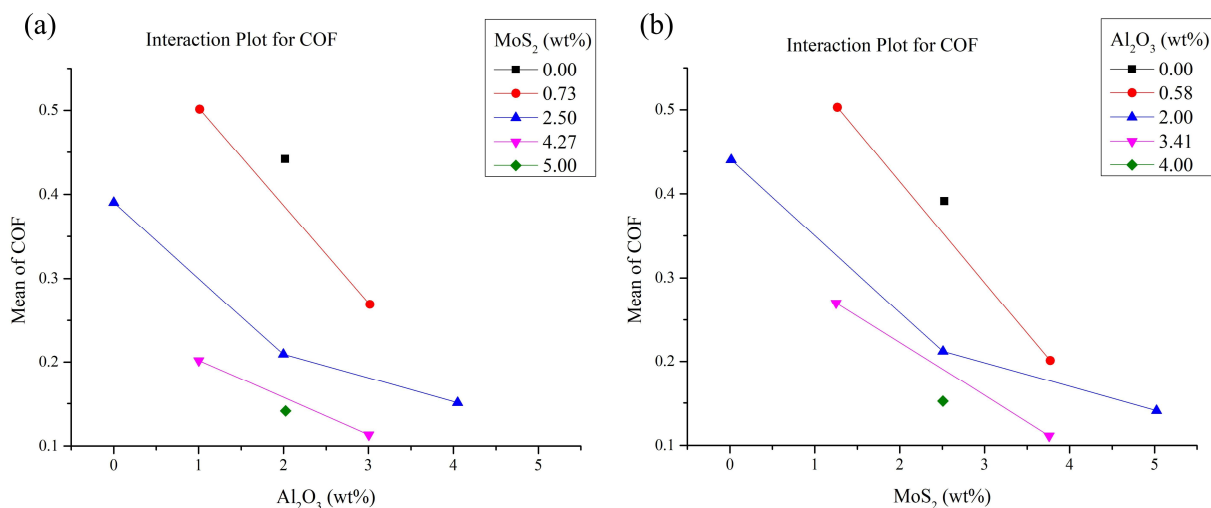


**Figure 4.** Interaction plot for COF. (a) Change in COF by adding Al<sub>2</sub>O<sub>3</sub> in constant amounts of MoS<sub>2</sub>. (b) Change in COF by adding MoS<sub>2</sub> in constant amounts of Al<sub>2</sub>O<sub>3</sub>.

As shown in Figure 5, incorporating nano- and microadditives into the epoxy resin reduces the COF. The lowest value of 0.12, with 98.3% accuracy, was achieved by adding 3.15 wt% nano-Al<sub>2</sub>O<sub>3</sub> and 4.44 wt% MoS<sub>2</sub> particles to an epoxy resin modified with 0.5 wt% GO.

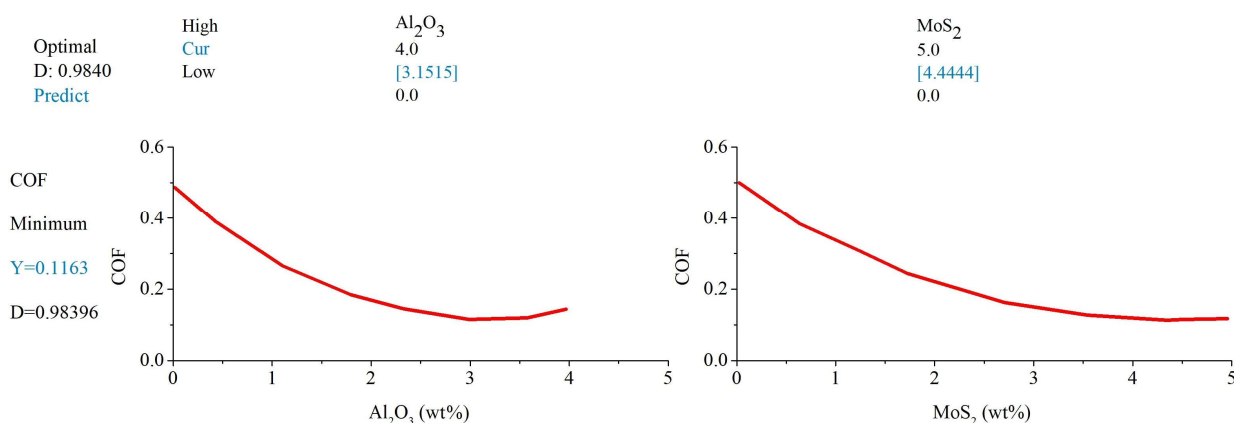


**Figure 5.** Optimization of additives for the lowest value of COF.

### 3.2.2. ANOVA analysis and model fitting for the wear rate of epoxy resin

The wear rate of the epoxy resin was significantly reduced by the addition of GO, nano-Al<sub>2</sub>O<sub>3</sub>, and MoS<sub>2</sub> particles, decreasing from  $180 \times 10^{-6}$  to  $2.5 \times 10^{-6}$  mm<sup>3</sup>/N·m, indicating that these additives

were highly effective in enhancing the tribological performance. Table 6 shows the ANOVA for the response surface model of wear rate. The analysis indicates that the terms  $\text{Al}_2\text{O}_3$ ,  $\text{MoS}_2$ , and  $\text{MoS}_2 \times \text{Al}_2\text{O}_3$  have a significant effect on the wear rate. The  $R^2$  and  $R^2$  (adj) values of 0.9984 and 0.9972 suggest that the model is sufficient without requiring additional tests.

**Table 6.** Analysis of variance for wear rate.

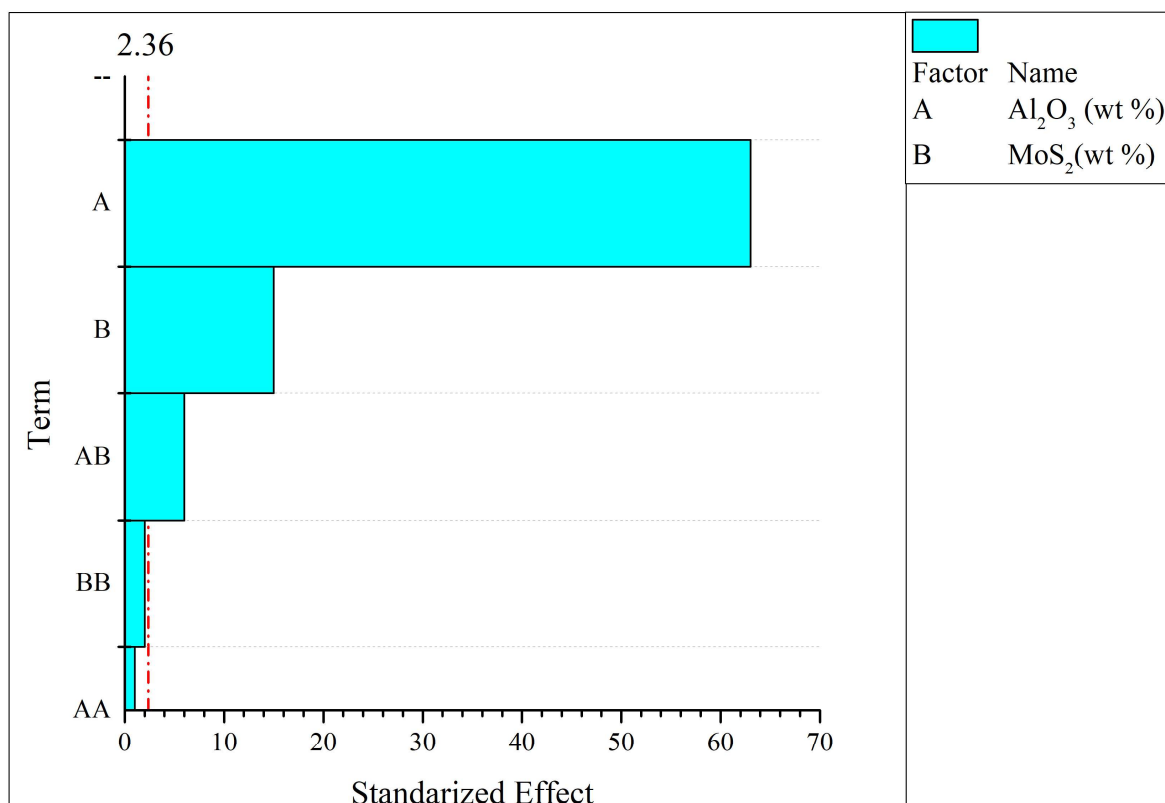
Source	DF <sup>(1)</sup>	Adj SS <sup>(2)</sup>	Adj MS <sup>(3)</sup>	F-value	P-value	
Model	5	6256.40	1251.28	860.53	0.001	
Linear	2	6204.43	3102.21	2133.44	0.001	
$\text{Al}_2\text{O}_3$	1	5960.08	5960.08	4098.84	0.001	Highly significant
$\text{MoS}_2$	1	244.35	244.35	168.04	0.001	Highly significant
Square	2	9.72	4.86	3.34	0.096	
$\text{Al}_2\text{O}_3 \times \text{Al}_2\text{O}_3$	1	0.50	0.50	0.35	0.575	Non-significant
$\text{MoS}_2 \times \text{MoS}_2$	1	8.51	8.51	5.85	0.046	Significant
2-way interaction	1	42.25	42.25	29.06	0.001	
$\text{Al}_2\text{O}_3 \times \text{MoS}_2$	1	42.25	42.25	29.06	0.001	Significant
Error	7	10.18	1.45			
Lack-of-fit	3	7.98	2.66	4.84	0.081	Non-significant
Pure error	4	2.20	0.55			
Total	12	6266.58				

Note: (1): Degrees of freedom; (2): adjusted sum of squares; (3): adjusted mean square. Model summary:  $R^2$ , 0.9984;  $R^2$  (adj), 0.9972.

The model above was used to predict the wear rate of the nano-epoxy composites. It can be expressed in terms of coded factors is presented in Eq 5:

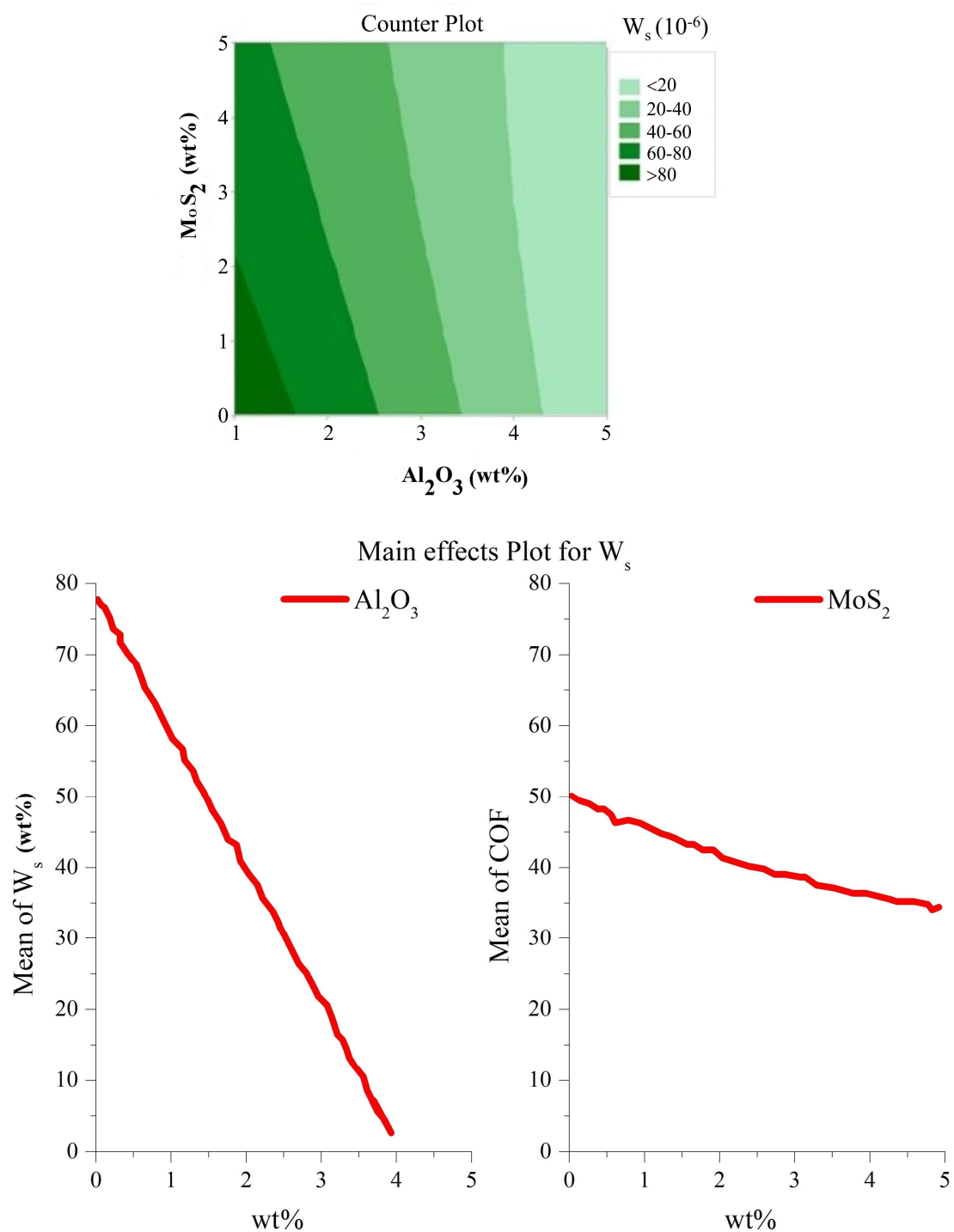
$$\text{Wear rate } (\times 10^{-6} \text{ mm}^3/\text{N}\cdot\text{m}) = 94.69 - 22.01 \text{ Al}_2\text{O}_3 - 7.496 \text{ MoS}_2 - 0.134 \text{ Al}_2\text{O}_3 \times \text{Al}_2\text{O}_3 + 0.354 \text{ MoS}_2 \times \text{MoS}_2 + 1.300 \text{ Al}_2\text{O}_3 \times \text{MoS}_2 \quad (5)$$

Eq 5 and Figure 6 show that the most significant factors affecting wear rate are  $\text{Al}_2\text{O}_3$ ,  $\text{MoS}_2$ , and  $\text{Al}_2\text{O}_3 \times \text{MoS}_2$ .



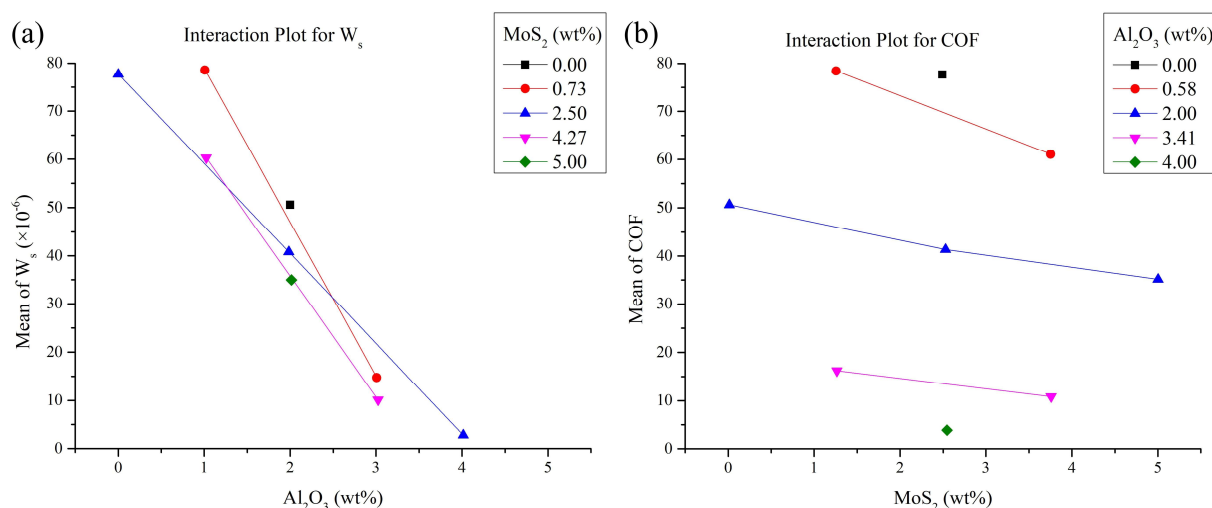
**Figure 6.** Pareto chart of the standardized effects on wear rate.

The variation of wear rate for different amounts of nano-Al<sub>2</sub>O<sub>3</sub> and MoS<sub>2</sub> was analyzed using contour plots and main effect plots (Figure 7). The contour plot illustrates the wear rate for all combinations of additive concentrations. For example, the wear rate can be reduced below  $20 \times 10^{-6} \text{ mm}^3/\text{N}\cdot\text{m}$  by adding 3.6 wt% nano-Al<sub>2</sub>O<sub>3</sub> and 0.5 wt% MoS<sub>2</sub>. The main effects plot shows that increasing MoS<sub>2</sub> content beyond 4 wt% does not significantly affect wear rate, whereas nano-Al<sub>2</sub>O<sub>3</sub> particles are very effective.



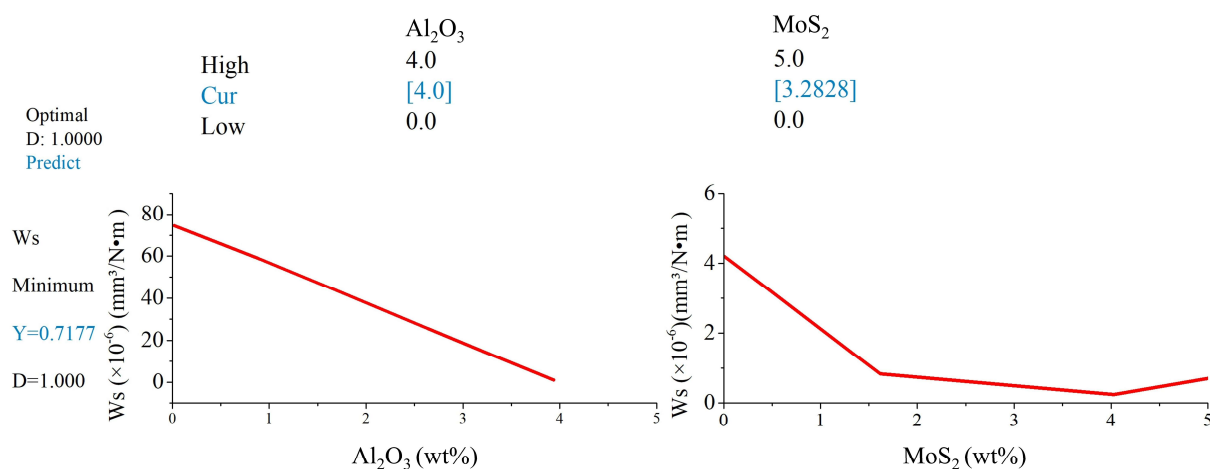
**Figure 7.** Contour plot and main effect plot for wear rate.

Figure 8 shows that the addition of 0.73 wt% MoS<sub>2</sub> with different Al<sub>2</sub>O<sub>3</sub> amounts leads to a drastically reduced wear rate to less than  $20 \times 10^{-6} \text{ mm}^3/\text{N}\cdot\text{m}$ .



**Figure 8.** Interaction plot for wear rate. (a) Variation of wear rate in response to the addition of  $Al_2O_3$  with constant amounts of  $MoS_2$ . (b) Variation of wear rate in response to the addition of  $MoS_2$  with constant amounts of  $Al_2O_3$ .

Figure 9 shows that the lowest value of wear rate,  $0.72 \times 10^{-6} \text{ mm}^3/\text{N}\cdot\text{m}$ , is obtained by adding 4 wt% nano- $Al_2O_3$  and 3.28 wt%  $MoS_2$  to epoxy resin modified with 0.5 wt% GO.



**Figure 9.** Optimization of additives for the lowest value of wear rate ( $\times 10^{-6} \text{ mm}^3/\text{N}\cdot\text{m}$ ).

### 3.2.3. Interpretation of results for wear rate and COF

Effect of nano- $Al_2O_3$  particles on wear rate and COF: nano- $Al_2O_3$  particles form a continuous transfer film on the sliding counterpart and enhance bonding between the film and the counterface. This reduces the wear rate of materials by maintaining consistent contact between the transfer film and the nanocomposite [18].

Effect of  $MoS_2$  particles on wear rate and COF:  $MoS_2$ , with its lamellar structure, exhibits low friction under certain conditions and is therefore widely used as a solid lubricant [1].

Figure 10 shows that some resin was transferred from the composite to the steel surface, and the presence of  $\text{MoS}_2$  effectively prevents adhesion between the steel and the resin counterpart [13].

The bonding provided by GO holds the  $\text{Al}_2\text{O}_3$  and  $\text{MoS}_2$  particles tightly in place. When the slippery  $\text{MoS}_2$  layers wear off during use, the tough base layer ( $\text{GO} + \text{Al}_2\text{O}_3$ ) continuously provides resistance to surface wear. Hard  $\text{Al}_2\text{O}_3$  particles protect the surface from damage, while GO acts as a net that prevents crack propagation through the material.

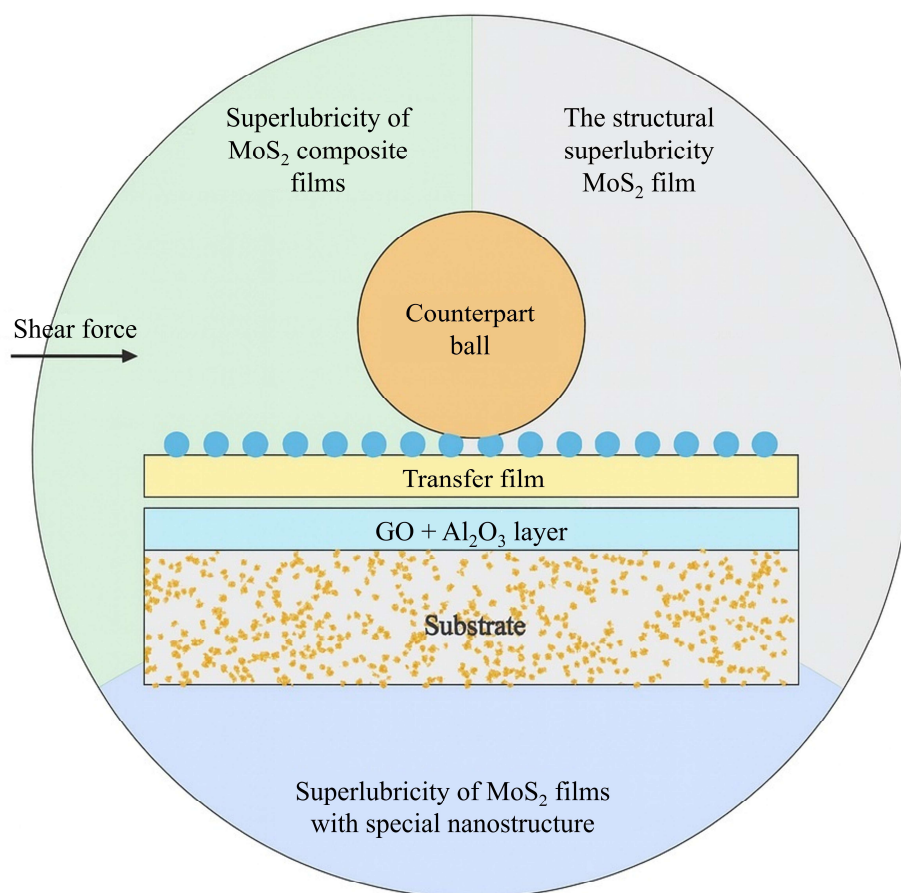


**Figure 10.** Tribology behavior of  $\text{MoS}_2$ .

#### 3.2.4. Optimization of additive composition for enhanced tribological performance

Analysis of the experimental data and modeling results by Minitab software indicated minimal residuals, as predicted values closely follow the diagonal line, confirming the reliability of the model. Figure 11 demonstrates that the optimum concentrations of nano- $\text{Al}_2\text{O}_3$  and  $\text{MoS}_2$  for tribological performance are 3.92 wt% and 3.99 wt%, respectively, resulting in:

- Coefficient of friction: 0.12
- Wear rate:  $2.3 \times 10^{-6} \text{ mm}^3/\text{N}\cdot\text{m}$

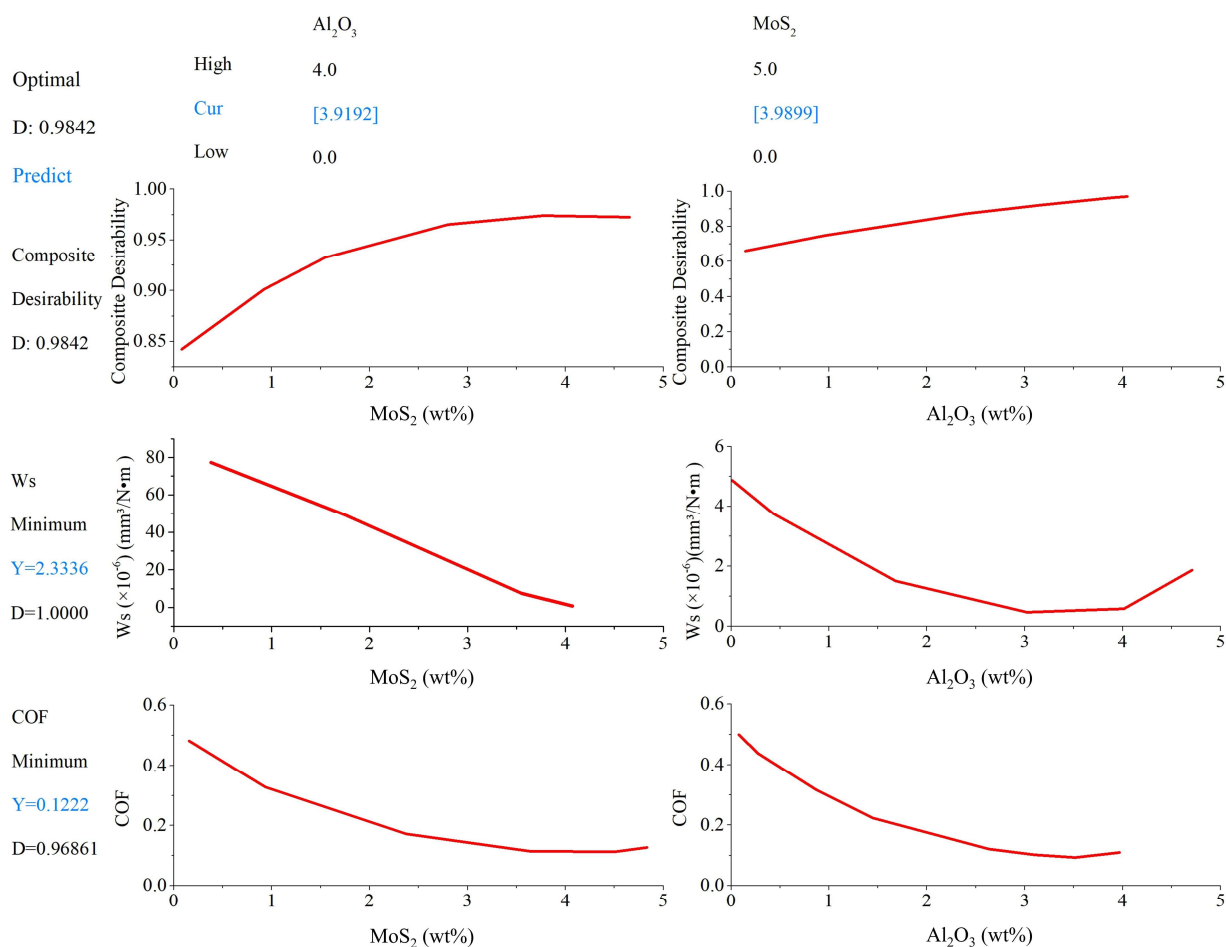


**Figure 11.** Optimization of additives for tribological properties.

We conducted tests on the optimal quantities to evaluate tensile strength, modulus of elasticity, and the convergence of the model with experimental results for tribological properties. These results are summarized in Table 7. The optimal composite (0.5 wt% GO, 3.92 wt% Al<sub>2</sub>O<sub>3</sub>, and 3.99 wt% MoS<sub>2</sub>) retained good mechanical properties, with a tensile strength of 75.4 MPa and a modulus of elasticity of 3.1 GPa. This represents a significant improvement over the unfilled epoxy (Table 3), with a 16% increase in tensile strength (from 65 to 75.4 MPa) and a 19% increase in modulus (from 2.6 to 3.1 GPa).

**Table 7.** Optimization of epoxy resin, graphene oxide, nano-Al<sub>2</sub>O<sub>3</sub>, and MoS<sub>2</sub> particles for different performance.

M	COF	Wear rate (mm <sup>3</sup> /N·m)	Tensile strength (MPa)	Modulus of elasticity (GPa)	Epoxy resin (g)	GO (wt%)	Al <sub>2</sub> O <sub>3</sub> (wt%)	MoS <sub>2</sub> (wt%)
1	0.118 (97.5%)*	2.27 × 10 <sup>-6</sup> (97.2%)*	75.4 (excellent)	3.1 (excellent)	100	0.5	3.63	4.04

\*Note: Matching percentage:  $[1 - (|0.1222 - 0.118| / 0.118)] \times 100\% \approx 97.5\%$ .



### 3.3. Analysis of the worn surface by scanning electron microscope (SEM)

SEM analysis of the worn surfaces provides critical insights into the wear-reduction mechanisms and the role of multi-scale fillers in the hybrid composite (epoxy/0.5% GO/3.92%  $\text{Al}_2\text{O}_3$ /3.99%  $\text{MoS}_2$ ). Figure 12 illustrates three primary wear mechanisms in the optimal nano-epoxy composite: abrasive wear (A), fatigue (B), and adhesive wear (C).

Abrasive wear occurs when hard particles slide across the surface, causing delamination and fatigue cracking. Under high contact pressure, surfaces adhere, and stress conditions change, activating fatigue mechanisms during repeated loading. This accelerates material loss. Additionally, high pressure generates elevated surface temperatures, further activating adhesive wear mechanisms.

The analysis reveals that filler particles detach from the matrix, creating fine debris that can move across the surface via scratching and rolling motions. Crack propagation depends on filler strength: cracks bypass strong particles but penetrate weak ones. Our results confirm that strong nanoparticle–epoxy bonding significantly resists surface degradation and minimizes material loss.

The additives mitigate wear by forming protective tribofilms that reduce direct surface contact. Hard particles resist abrasion and carry load, while solid lubricants minimize friction and prevent adhesive wear and surface fatigue.

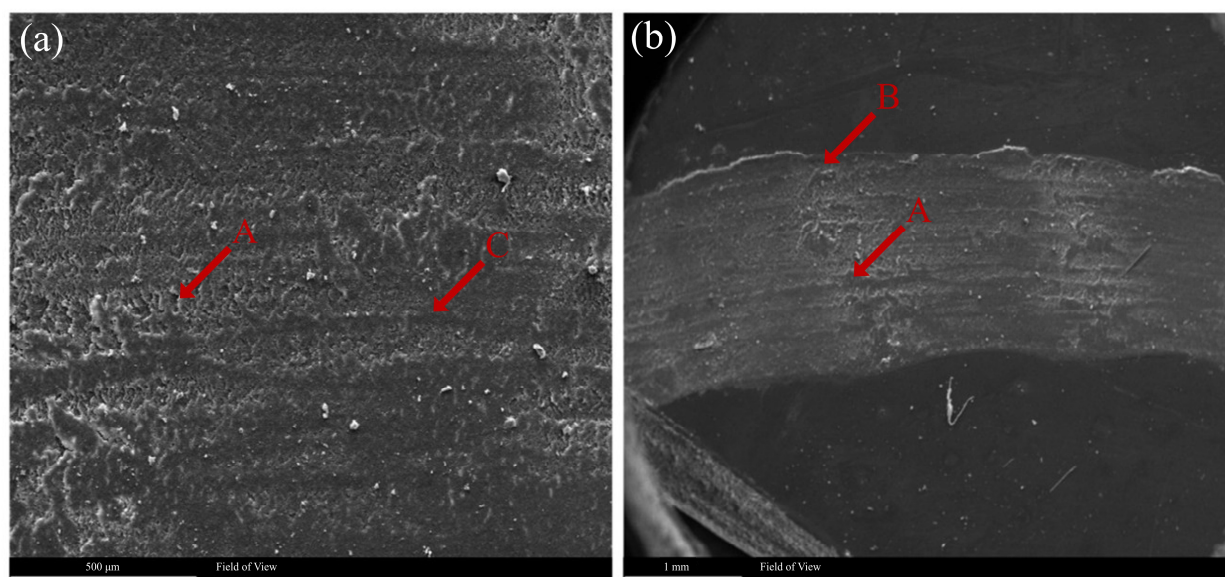


**Figure 12.** SEM of the worn surface for the nano-epoxy composite specimen: (a) 500  $\mu\text{m}$  and (b) 1 mm.

## 4. Conclusions

To enhance the tribological performance of Araldite LY 5052 epoxy resin, hybrid nanocomposites were fabricated by incorporating GO, nano- $\text{Al}_2\text{O}_3$ , and  $\text{MoS}_2$  particles. An initial fixed amount of 0.5 wt% GO was added to the epoxy based on preliminary findings that indicated its effectiveness in improving mechanical and tribological properties. Subsequently, a surface response methodology (design of experiments, DoE) was employed to determine the optimal weight percentages of nano- $\text{Al}_2\text{O}_3$  (0–4 wt%) and  $\text{MoS}_2$  (0–5 wt%) particles. A total of thirteen

experimental tests were conducted, and the resulting data were analyzed using Minitab software to generate predictive models.

The analysis demonstrated a significant synergistic effect between GO, nano-Al<sub>2</sub>O<sub>3</sub>, and MoS<sub>2</sub> particles, leading to a substantial improvement in the coefficient of friction and wear rate.

The optimal formulation for superior tribological performance was identified as follows:

- 0.5 wt% GO
- 3.92 wt% nano-Al<sub>2</sub>O<sub>3</sub>
- 3.99 wt% MoS<sub>2</sub>

This optimal blend yielded the following responses:

- Coefficient of friction: 0.12
- Wear rate:  $2.3 \times 10^{-6} \text{ mm}^3/\text{N}\cdot\text{m}$

Further analysis of the models revealed that MoS<sub>2</sub> particles had a more pronounced effect on reducing the coefficient of friction, while nano-Al<sub>2</sub>O<sub>3</sub> particles contributed more significantly to enhancing wear resistance. Experimental data were successfully modeled into regression equations, enabling the prediction of the epoxy resin's behavior across a range of additive concentrations.

The results confirm that the development of a self-lubricating epoxy composite with significantly enhanced tribological properties is achievable through the strategic hybridization of GO, nano-Al<sub>2</sub>O<sub>3</sub>, and MoS<sub>2</sub> particles.

### Use of AI tools declaration

The author declares that no artificial intelligence (AI) tools were used in the creation of this article.

### Acknowledgments

The support of Diyala University is acknowledged.

### Conflict of interest

The author declares no conflict of interest.

### References

1. Menezes PL, Rohatgi PK, Omrani E (2018) *Self-Lubricating Composites*, Heidelberg: Springer Berlin. <https://doi.org/10.1007/978-3-662-64243-6>
2. Friedrich K, Schlarb AK (2008) *Tribology of Polymeric Nanocomposites: Friction and Wear of Bulk Materials and Coatings*, Oxford: Butterworth-Heinemann. <https://doi.org/10.1016/C2011-0-09093-2>
3. Ratna D, Chakraborty BC (2024) Chapter 1. Introduction to composite materials, In: Ratna D, Chakraborty BC, *Polymer Matrix Composite Materials: Structural and Functional Applications*, Berlin, Boston: De Gruyter, 1–72. <https://doi.org/10.1515/9783110781571-001>
4. Hutchings I, Shipway P (2017) *Tribology: Friction and Wear of Engineering Materials*, Oxford: Butterworth-Heinemann. <https://www.sciencedirect.com/book/9780081009109/tribology>

5. Omrani E, Rohatgi PK, Menezes PL (2019) *Tribology and Applications of Self-Lubricating Materials*, Boca Raton: CRC Press. <https://doi.org/10.1201/9781315154077>
6. Delogu F, Gorrasi G, Sorrentino A (2017) Fabrication of polymer nanocomposites via ball milling: Present status and future perspectives. *Prog Mater Sci* 86: 75–126. <https://doi.org/10.1016/j.pmatsci.2017.01.003>
7. Davim JP (2013) *Tribology of Nanocomposites*, Heidelberg: Springer Berlin. <https://doi.org/10.1007/978-3-642-33882-3>
8. Kurahatti RV, Surendranathan AO, Kumar AVR, et al. (2014) Dry sliding wear behaviour of epoxyreinforced with nanoZrO<sub>2</sub> particles. *Procedia Mater Sci* 5: 274–280. <https://doi.org/10.1016/j.mspro.2014.07.267>
9. Monteserín C, Blanco M, Aranzabe E, et al. (2017) Effects of graphene oxide and chemically-reduced graphene oxide on the dynamic mechanical properties of epoxy amine composites. *Polymers* 9: 449. <https://doi.org/10.3390/polym9090449>
10. Wang Q, Xue Q, Liu H, et al. (1996) The effect of particle size of nanometer ZrO<sub>2</sub> on the tribological behaviour of PEEK. *Wear* 198: 216–219. [https://doi.org/10.1016/0043-1648\(96\)07201-8](https://doi.org/10.1016/0043-1648(96)07201-8)
11. Chang L, Zhang Z (2006) Tribological properties of epoxy nanocomposites: Part II. A combinative effect of short carbon fibre with nano-TiO<sub>2</sub>. *Wear* 260: 869–878. <https://doi.org/10.1016/j.wear.2005.04.002>
12. Shi G, Zhang MQ, Rong MZ, et al. (2003) Friction and wear of low nanometer Si<sub>3</sub>N<sub>4</sub> filled epoxy composites. *Wear* 254: 784–796. [https://doi.org/10.1016/S0043-1648\(03\)00190-X](https://doi.org/10.1016/S0043-1648(03)00190-X)
13. Chen B, Ni BJ, Fu MX, et al. (2019) Effect of molybdenum disulfide exfoliation conditions on the mechanical properties of epoxy nanocomposites. *Chin J Polym Sci* 37: 687–692. <https://doi.org/10.1007/s10118-019-2239-7>
14. Tang LC, Wan YJ, Yan D, et al. (2013) The effect of graphene dispersion on the mechanical properties of graphene/epoxy composites. *Carbon* 60: 16–27. <https://doi.org/10.1016/j.carbon.2013.03.050>
15. El-Ghazaly A, Anis G, Salem HG (2017) Effect of graphene addition on the mechanical and tribological behavior of nanostructured AA2124 self-lubricating metal matrix composite. *Compos Part A Appl Sci Manuf* 95: 325–336. <https://doi.org/10.1016/j.compositesa.2017.02.006>
16. ASTM International (2017) Standard test method for wear testing with a pin-on-disk apparatus. ASTM G99-17.
17. Berman D, Erdemir A, Sumant AV (2014) Graphene: A new emerging lubricant. *Mater Today* 17: 31–42. <https://doi.org/10.1016/j.mattod.2013.12.003>
18. Stachowiak GW, Batchelor AW (1993) *Engineering Tribology*, Boston: Butterworth-Heinemann. <https://doi.org/10.1016/C2011-0-07515-4>



AIMS Press

© 2025 the Author(s), licensee AIMS Press. This is an open access article distributed under the terms of the Creative Commons Attribution License (<https://creativecommons.org/licenses/by/4.0>)